Editors' Suggestion

Dark Matter Induced Power in Quantum Devices

Anirban Das,[1,*] Noah Kurinsky,[1,2,†] and Rebecca K. Leane[1,2,‡]
[1]SLAC National Accelerator Laboratory, 2575 Sand Hill Road, Menlo Park, California 94025, USA
[2]Kavli Institute for Particle Astrophysics and Cosmology, Stanford University, Stanford, California 94035, USA

(Received 2 November 2022; revised 19 January 2024; accepted 21 February 2024; published 22 March 2024)

We point out that power measurements of single quasiparticle devices open a new avenue to detect dark matter (DM). The threshold of these devices is set by the Cooper pair binding energy, and is therefore so low that they can detect DM as light as about an MeV incoming from the Galactic halo, as well as the low-velocity thermalized DM component potentially present in the Earth. Using existing power measurements with these new devices, as well as power measurements with SuperCDMS-CPD, we set new constraints on the spin-independent DM scattering cross section for DM masses from about 10 MeV to 10 GeV. We outline future directions to improve sensitivity to both halo DM and a thermalized DM population in the Earth using power deposition in quantum devices.

DOI: 10.1103/PhysRevLett.132.121801

Introduction.—At any given moment, a powerful stream of dark matter (DM) particles from the Galactic halo flows into Earth. This Galactic DM has been extensively searched for in direct detection experiments, which aim to detect recoil events when DM scatters off the standard model (SM) target material, thereby providing a test of the DM-SM scattering cross section. Typically, the energy threshold of direct detection experiments assuming nuclear recoils is about a keV corresponding to the recoil expected for DM with mass above about a GeV for standard analyses [1], or MeV-scale masses when exploiting the Migdal effect [2–6] or electron recoils [7–9].

Given the lack of conclusive DM detection with direct detection experiments so far, interest in novel detection strategies and new devices has exploded in the last few years [10]. In particular, the race down to increasingly low thresholds has inspired the use of new detectors, including superconductors [11–16], superfluids [17–19], polar crystals [20–22], topological materials [23], and Dirac materials [24–27]. Superconductors show exceptional promise due to their superconducting energy gaps as low as about an meV, allowing probes of light DM.

The goal of lower threshold experiments to date has been to push down sensitivity to lower DM masses, and we will exploit this to test incoming halo DM down to the MeV scale. Lowered thresholds open up a new probe of a DM component other than the usually considered halo DM. When the Galactic halo DM enters Earth, it scatters, loses energy, and can become gravitationally captured. Over time, this builds up a thermalized population of DM particles bound to Earth. For DM around a few GeV that is in local thermal equilibrium, the density of bound DM at Earth's surface can in fact be enormous: about 15 orders of magnitude higher than the local DM halo density [28–36]. Unfortunately, this large density enhancement is lost on traditional direct detection experiments, as the bound DM population has a very low velocity compared to halo DM, requiring thresholds of less than about 0.05 eV at Earth's surface.

We will demonstrate for the first time that power measurements using new quantum devices can be used to detect DM with low-energy depositions. This includes sensitivity to both light DM from the halo, as well as thermalized bound DM. As schematically shown in Fig. 1, for thermalized DM our proposal exploits their high DM density and is sufficiently sensitive despite low thermal velocities compared to traditional direct detection, which only measures the less frequent and higher-velocity DM halo interactions. We point out and will use the fact that both

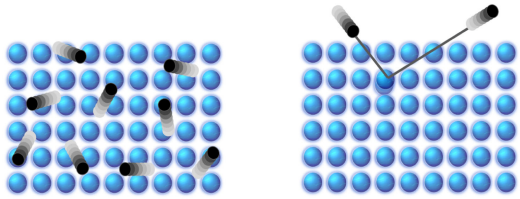

FIG. 1. The qualitative difference between our proposal and a conventional DM direct detection experiment. The noise arises from frequent interaction between DM and the nuclei in the detector, as opposed to once-in-a-while recoil of a nucleus from DM scattering.

halo DM and thermalized DM would produce excess quasiparticle generation in single quasiparticle devices, and excess power produced in athermal phonon sensors, to set new constraints on DM with interaction cross sections larger than about 10^{-34}–10^{-28} cm^2 for DM masses of ∼300 MeV to 10 GeV for thermalized DM. For halo DM, we will set constraints down to about 10^{-29}–10^{-26} cm^2 for DM masses of ∼10 MeV to 10 GeV.

Dark matter at Earth's surface.—At Earth's position, there are two potential DM components present, which have different DM velocity and density assumptions. We will test both of these components. One is DM incoming from the Galactic halo, which is usually assumed for direct detection experiments. The other is the thermalized DM component. This thermalized component exists, as once DM enters Earth, it can thermalize and become captured and bound to Earth. For sufficiently large DM-SM scattering cross sections (larger than about 10^{-35} cm^2), the DM rapidly thermalizes and is said to be in local thermal equilibrium with the surrounding SM matter. In this case, the DM radial profile within Earth n_χ is dominantly governed by the differential equation [36]

$$\frac{\nabla n_\chi}{n_\chi} + (\kappa + 1)\frac{\nabla T}{T} + \frac{m_\chi g}{T} = \frac{\Phi}{n_\chi D_{\chi N}}\frac{R_\oplus^2}{r^2}, \tag{1}$$

where T is Earth's radial temperature profile at position r, $R_\oplus$ is Earth's radius, m_χ is the DM mass, g is gravitational acceleration, and Φ is the incoming flux of DM particles from the Galactic halo. $D_{\chi N} \sim \lambda v_{\rm th}$ and $\kappa \sim -1/[2(1 + m_\chi/m_{\rm SM})^{3/2}]$ are diffusion coefficients [36], with λ the DM mean free path, $v_{\rm th}$ the DM thermal velocity, and $m_{\rm SM}$ the SM target mass. The DM density profile is normalized by enforcing that its volume integral equals the total number of particles expected within Earth [36].

Solving Eq. (1) for $n_\chi(r)$ reveals that this thermalized population of DM can be significantly more abundant at Earth's surface than the incoming halo DM particles. For DM masses around a GeV, the local DM density can be as high as $\sim 10^{14}$ cm^{-3}. However, as this population is thermalized within Earth, its velocity is low. We approximate the thermalized DM velocity distribution as a truncated Maxwell-Boltzmann distribution,

$$f_\chi(\boldsymbol{v}) = \frac{1}{N_0} e^{-(v/v_{\rm th})^2}\Theta(v_{\rm esc} - v), \tag{2}$$

where N_0 normalizes the distribution, and $v_{\rm th}^2 = 8T_\chi/\pi m_\chi$ with $T_\chi \simeq 300$ K. This velocity would require thresholds of $E \lesssim 0.05$ eV for conventional detection techniques. This is much lower than the reach of typical direct detection experiments, and so it requires new techniques to be detected. Our assumption of DM being at room temperature of ∼300 K is reasonable, as even at the largest cross sections considered, the mean free path is much larger than the size of our devices, such that DM is not expected to thermalize with the device itself.

For halo DM, in Eq. (2) $v_{\rm th}$ is replaced by the average DM velocity in the halo $v_0 = 230$ km/s. In this case, the relative velocity between Earth and DM also becomes important. Hence, for halo DM we use the boosted velocity $\boldsymbol{v} \to \boldsymbol{v} + \boldsymbol{v}_\oplus$ in Eq. (2), where $|\boldsymbol{v}_\oplus| = 240$ km/s is Earth's velocity in the Galactic rest frame. The halo DM density is assumed to be 0.4 GeV cm^{-3}. We now show that quantum devices are highly sensitive to DM with low-energy depositions through their power measurements, which includes both the thermalized DM population, as well as light halo DM.

Scattering rate and energy deposition.—As a DM particle with velocity $\boldsymbol{v}$ scatters in the detector and transfers momentum $\boldsymbol{q}$, it deposits an amount of energy

$$\omega_{\boldsymbol{q}} = \boldsymbol{q}\cdot\boldsymbol{v} - \frac{q^2}{2m_\chi} = E_f - E_i. \tag{3}$$

As a result, the target makes a transition from $|i\rangle$ to $|f\rangle$. For such low-energy depositions, the momentum transferred is comparable to the inverse size of a nuclear wave function in a detector crystal, and the interatomic forces become important. Hence, lattice vibrations or phonon excitations will be used to compute the DM scattering rate. The total rate per unit target mass can be written as [37,38]

$$\Gamma = \frac{\pi\sigma_{\chi N} n_\chi}{\rho_T \mu^2}\int d^3v f_\chi(\boldsymbol{v}) \int \frac{d^3q}{(2\pi)^3} F_{\rm med}^2(q) S(\boldsymbol{q}, \omega_{\boldsymbol{q}}). \tag{4}$$

Here, $f_\chi(\boldsymbol{v})$ is the DM velocity distribution, ρ_T is the target density, $\sigma_{\chi N}$ is the DM-nucleon scattering cross section, μ is the reduced mass of the DM-nucleon system, $F_{\rm med}(q)$ is a form factor that depends on the mediator [we assume $F_{\rm med}(q) = 1$], and $S(\boldsymbol{q}, \omega_{\boldsymbol{q}})$ is the dynamic structure factor containing the detector response to DM scattering and depends on the crystal structure of the target material.

To compute DM scattering rates, we follow Refs. [39,40] and use the publicly available code DarkELF. We modify DarkELF in two main ways. First, we update the local DM density and DM velocity input to be that described in the previous section, for halo or thermalized DM as appropriate. Second, the code was developed only for materials with two atoms per primitive cell, which is the smallest crystal unit. Thus, we adapt it for materials like Al which has only one atom in its primitive cell.

Detection mechanisms and materials.—Detecting light halo DM or the captured DM population of low thermal energy demands the use of low threshold quantum sensors that can detect $\sim\mathcal{O}(10)$ meV energy deposition. Such sensors are usually designed using superconducting materials, which have small energy gaps [41–44]. Al is a widely used superconductor for such a purpose, and its characterization data are readily available. Such a small amount of

energy transfer is not sufficient for nuclear recoil or electronic ionization; however, DM can excite collective modes, such as phonons in the material, resulting in an excess power. For example, in one experimental setup, a bias circuit stabilizes the absorber material at its transition temperature T_c, where its resistance is very sensitive to any energy deposition. The total power deposited in the detector by DM in the form of phonons is

$$P_{\mathrm{DM}} = \epsilon \int d\omega\, \omega \frac{d\Gamma}{d\omega}, \tag{5}$$

where ϵ is an efficiency factor that depends on the experimental setup. We will use this to calculate excess power due to DM and set constraints on DM-SM interactions. Volume-scaled detectors based on conventional semiconductors, such as Si, can also be used as the absorber material to look for ambient power deposition; the power deposited per unit volume can be obtained from Eq. (5).

We also consider excess quasiparticle production from DM. In a superconducting metal, the electrons are bound into Cooper pairs through a long-range interaction with phonons. When a DM particle scatters with a nucleus, it may deposit its kinetic energy in the form of phonons. If the deposited energy exceeds the energy gap Δ of the superconductor, these excess phonons will break some of the Cooper pairs and release quasiparticles above the gap. We will therefore set limits on DM-SM interactions by calculating quasiparticle production rates from DM.

The quasiparticle generation rate R_{QP} by DM scattering can be written as

$$\begin{aligned} R_{\mathrm{QP}} &= \frac{\epsilon_{\mathrm{QP}}}{\Delta} \int d\omega\, \omega \frac{d\Gamma}{d\omega} \\ &\approx \left(\frac{P_{\mathrm{DM}}}{9 \times 10^{-23}\ \mathrm{W\,\mu m^{-3}}} \right) \mathrm{Hz\,\mu m^{-3}}, \end{aligned} \tag{6}$$

where P_{DM} is the deposited DM power above the gap in $\mathrm{W\,\mu m^{-3}}$, assuming a 60% quasiparticle generation efficiency ($\epsilon_{\mathrm{QP}} = 0.6$) [14,45], and using $\Delta \simeq 340$ μeV for Al.

A conservative estimate of n_{QP}, the steady-state quasiparticle density, can be found using the mean field results from Ref. [46] as follows:

$$\frac{dn_{\mathrm{QP}}}{dt} = -\Gamma_R - \Gamma_T + A \approx -\bar{\Gamma} n_{\mathrm{QP}}^2 - \bar{\Gamma}_T n_{\mathrm{QP}} + A, \tag{7}$$

with Γ_R, Γ_T, A the recombination, trapping, and generation rates, respectively. With a steady-state injected power density P, we have $A = P/(2\Delta)$ where Δ is the gap energy. In equilibrium, we thus find

$$P/(2\Delta) = \bar{\Gamma} n_{\mathrm{QP}}^2 + \bar{\Gamma}_T n_{\mathrm{QP}}. \tag{8}$$

The mean field calculation assumes no trapping of QPs with $\bar{\Gamma}_T = 0$, which leads to the relation $n_{\mathrm{QP}} = \sqrt{A/\bar{\Gamma}} \propto \sqrt{P}$. In the case of DM scattering, $A = R_{\mathrm{QP}}$ using Eq. (6), and $\bar{\Gamma} = 40\ \mathrm{s^{-1}\,\mu m^3}$ for Al. The steady-state density is therefore

$$n_{\mathrm{QP}} \approx \left(\frac{P_{\mathrm{DM}}}{3.6 \times 10^{-21}\ \mathrm{W}} \right)^{1/2} \mathrm{\mu m^{-3}}, \tag{9}$$

which can be compared to known measurements to set new constraints. We now discuss devices that can be used to detect DM using power deposition.

Detecting dark matter with single quasiparticle devices.—(i) Quasiparticle tunneling in transmon qubits. It is important to minimize quasiparticle excitations formed from broken Cooper pairs in quantum devices, as the quasiparticle background limits the operation of applications such as radiation detectors and superconducting qubits. To study the effect of quasiparticle tunneling on the decoherence of a transmon qubit, Ref. [41] constructed a single junction superconducting qubit made of Al and studied its decoherence by monitoring the single-charge tunneling rate. From the observed relaxation rate of the qubit, they found a quasiparticle density of $0.04 \pm 0.01\ \mathrm{\mu m^{-3}}$ with a thermalized distribution [41].

We convert this measurement to a power density using Eq. (9), finding an upper limit of $3.92 \times 10^{-24}\ \mathrm{W\,\mu m^{-3}}$. We compare this directly with the expected DM induced quasiparticle density in Al and consider this an upper limit on residual power injection. Moreover, the source of this quasiparticle density is not known and usually assigned to the background radiation from the environment [41]. Therefore, it is possible that the DM scattering contributes to it too. We overall point out that quasiparticles produced by DM, and therefore the DM-SM scattering rate, can be probed using devices with low-quasiparticle density backgrounds.

(ii) Low-noise bolometers. Understanding our Universe deep into the infrared would reveal new secrets of galaxy formation, exoplanets, and so much more. However, far-infrared spectroscopy requires new cryogenic space telescopes with technologies capable of measuring very cold objects, and therefore require low-noise equivalent power in their detectors. Adapting technology from quantum computing applications, Ref. [42] developed a quantum capacitance detector where photon-produced free electrons in a superconductor tunnel into a small capacitive island. This setup is embedded in a resonant circuit, and therefore can be referred to as a "quantum resonator." This quantum resonator measured excess power of 4×10^{-20} W [42], making it the most sensitive existing far-infrared detector. The volume of the absorber used in this case was a mesh grid, roughly 60 microns square with a 1% fill factor and 60 nm thick. This corresponds to a volume of around $1.56\ \mathrm{\mu m^3}$ and thus a power density measurement of $2.6 \times 10^{-20}\ \mathrm{W\,\mu m^{-3}}$. We therefore point out that single quasiparticle devices can

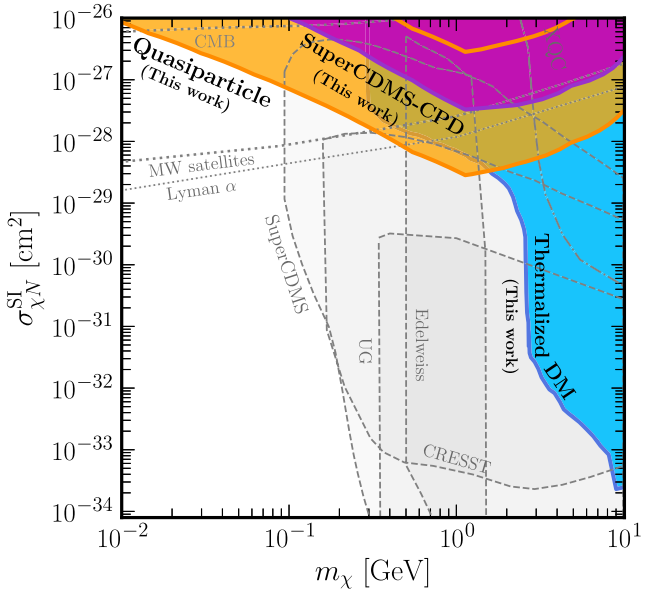

FIG. 2. New limits on spin-independent DM-nucleon scattering cross section $\sigma_{\chi N}$ derived in this work, using quantum devices. We show halo DM limits from quasiparticle production measurement (orange) and SuperCDMS-CPD (magenta). "Thermalized DM" (blue) is our new constraint on the thermalized DM population, with several experiments overlapping in their exclusion of this population. The gray regions are other existing limits; see text for discussion.

be used for DM detection through their power measurements, and will use this current measurement to set constraints on the DM-SM scattering rate which would produce excess power. Note that this detector has a calibrated photon detection efficiency of greater than 95%, which reduces the systematic uncertainty on the power limit. Reference [42] excludes the possibility that this is induced by residual radiation and represents a true, measured excess power.

For both devices above, we will only consider DM detection from the superconductor films, rather than the substrate. In the case of the transmon qubit, it is a conservative choice. While for the bolometer, the substrate is connected to the ground plane made of metallic Au-Ti, which acts as a phonon trap stopping the phonons created in the substrate from traveling into Al; see the Supplemental Material [47] for more details.

Detecting DM power deposition with existing DM detectors.—While we have pointed out new devices that can be used as DM detectors above, we also point out that more conventional quantum sensors with volume scaling can already be used to constrain low-energy deposition DM through their power measurements. We consider SuperCDMS detectors, which have recorded volume-scaled transition-edge sensor (TES) bias power measurements in which the TES is coupled to a large aluminum absorber [44]. For Ref. [44], we find a bias power of 2×10^{-15} fW, and an Al absorber with a volume of 2×10^6 μm^3. This yields a power density of order 10^{-21} W μm^{-3}. The coupling efficiency of power to the readout in this case is 30% ($\epsilon = 0.3$), so our bound on DM power using Al would be 3×10^{-21} W μm^{-3}. However, the best constraints on DM scattering power injection come from SuperCDMS-CPD [43], which instead has 10.6 g of Si as the absorber material. In this case, an excess power of 6 pW was measured in the phonon sensor arrays, corresponding to an excess substrate power of 18 pW or 10^{-24} W μm^{-3}. As this provides the superior limit, we use the measurement from SuperCDMS-CPD [43]. Using the Si as the sole absorber volume in the phonon calorimeter device used in SuperCDMS is justified because its design was optimized to maximize the collection of phonons from the Si block into the superconducting Al fins; see the Supplemental Material [47] for further discussion. Note that in Ref. [35], future projections with a hypothetically altered version of SuperCDMS were considered for thermalized DM. Here, we already use the current SuperCDMS measurements to set the first limits.

New dark matter constraints.—Figure 2 shows the new bounds we derive for spin-independent DM-SM scattering. The strongest sensitivity is achieved using quasiparticle density measurements. The conversion from the quasiparticle density to quasiparticle generation rate can only be trusted to an order of magnitude, so we show two orange "quasiparticle" lines representing a conservative and an optimistic constraint, which corresponds to taking $\bar{\Gamma} = 4$ or 400 s^{-1} μm^3, respectively, i.e., moving the quasiparticle generation rate between its expected range of validity. The next strongest bound arises from scattering power injection with SuperCDMS CPD shown in magenta, where we find that their volume advantage still overcomes the superior power sensitivity of the low-noise bolometer, which is too weak to show on the plot for halo DM. The top two bounds correspond to limits using the incoming halo DM, while the blue "thermalized DM" constraint uses only the thermalized DM population.

In Fig. 2, for thermalized DM, all three of our quantum devices overlap in their constraint strength. The thermalized DM curve is truncated not due to device sensitivity, but rather because DM evaporates to the left of the blue contour. This occurs due to thermal kicks transferring too much energy to the DM particle relative to the gravitational binding energy of Earth, such that DM escapes Earth and does not remain bound to produce any signal. If there was no DM evaporation, as is possible in models other than the purely contact cross section setup we considered here [48], the quantum sensors would have sensitivity extending to much lower cross sections for the thermalized DM component. This motivates further studies of models that do not evaporate at these DM masses and cross sections. In Fig. 2, for thermalized DM, largest DM densities are achieved for the asymmetric DM, which we assume for our densities,

though we are also sensitive to annihilating DM models; p-wave annihilating DM does also not affect our assumed DM densities [36]. Note that in comparison, the incoming halo DM limits do not require any assumptions about DM annihilation. The halo limits extend to lower masses, as incoming DM, which later evaporates, still leads to a bound from when DM is first entering Earth. We do not show ceilings for our limits, which will exist but require simulations to calculate accurately. We expect this could lower the limits at large cross sections at the top of Fig. 2. We focus on below 10 GeV in Fig. 2, as heavier DM more readily sinks farther into Earth, and so the sensitivity becomes weaker outside this mass range.

In Fig. 2, we also compare with existing limits, including those from astrophysical systems such as Milky Way satellites [49], Lyman-alpha [50], and the CMB [51]. There are also lab experiments overlapping part of our parameter space, namely, CRESST [52], SuperCDMS [53], Edelweiss [54], XQC [55], and "UG," which is a combined limit line from deep underground experiments [56–61]. However, there is significant ambiguity in the interpretation at cross sections exceeding about 10^{-30} cm^2 where the Born approximation breaks down, and the nuclear coherence across different detector materials is not well defined without using a DM model [62,63]. For transparency, we show all bounds that have been quoted in this parameter space, but emphasize many of these bounds are not generic, have different assumptions, and cannot be directly compared in a consistent manner without a DM model [62,63]. As such, our bounds significantly add to the picture of exclusions on this parameter space, even in the regions where they naively appear to overlap. There are also regions where we only overlap with astrophysical measurements, which are inherently less certain than our lab-based measurements. In addition, these astrophysical bounds disappear for models where the DM tested here is a subfraction of the total abundance of DM, while our bounds do not.

Conclusions and outlook.—We presented existing quantum sensors, which have so far not been used to search for DM, as new DM detectors. We pointed out for the first time that such devices allow a probe of DM through excess quasiparticle generation in single quasiparticle devices, and excess power produced in athermal phonon sensors. We considered DM power deposition in these devices, and their already existing measurements, to constrain two types of DM which potentially exist in the Earth. First, we constrained MeV-scale and higher DM masses from the incoming Galactic halo. Second, we set limits on the thermalized DM, which is already captured and thermalized within Earth, for MeV-GeV scale DM.

We identified these new DM sensitivities with three different devices. Single quasiparticle devices provide new constraints already, with promise to provide improved results in the future if lower background noise is achieved. The best limit arises from quasiparticle density measurements in devices aiming for low quasiparticle backgrounds. The quasiparticle density measurement we used from Ref. [41] may also bring new sensitivities in the future. For example, recently, Ref. [64] measured an even lower quasiparticle density in superconducting Al. However, we do not use their value because our model of quasiparticle tunneling is not applicable to their experimental setup. This is detailed further in the Supplemental Material [47]. We also set new constraints using volume-scaled TES bias power measurements, in which the TES is coupled to a large silicon absorber, as per the SuperCDMS detectors. In the future, a larger volume absorber measured with better systematic controls would be able to provide stronger sensitivities to thermal DM.

Interestingly, it is not known what currently produces the quasiparticles measured in these devices [64–68]. We thus conclude that, for plausible DM parameters, this signal could correspond to a DM signal if seen to remain fixed in time, but we caution that this requires proper studies of systematics which at this point are lacking, including an accurate model for relating power injection to quasiparticle generation as we discussed above.

Going forward, our work serves as strong motivation to better understand the systematic uncertainties corresponding to some of these measurements, and motivates further exploration with quantum devices to probe the highly abundant, low-velocity, thermalized DM population. Moreover, the encouraging results obtained here will inspire future study to optimize the absorber material for low-velocity DM detection.

We thank Simon Knapen, Tongyan Lin, Robert McDermott, Britton Plourde, Matt Pyle, and Juri Smirnov for helpful discussions and comments. A. D. and R. K. L. are supported by the U.S. Department of Energy under Contract No. DE-AC02-76SF00515. N. K. is supported by the U.S. Department of Energy Early Career Research Program under Grant No. FWP 100872.

*nirband@slac.stanford.edu
†kurinsky@slac.stanford.edu
‡rleane@slac.stanford.edu

[1] J. Aalbers *et al.* (LUX-ZEPLIN Collaboration), Phys. Rev. Lett. **131**, 041002 (2023).
[2] J. D. Vergados and H. Ejiri, Phys. Lett. B **606**, 313 (2005).
[3] C. C. Moustakidis, J. D. Vergados, and H. Ejiri, Nucl. Phys. **B727**, 406 (2005).
[4] R. Bernabei *et al.*, Int. J. Mod. Phys. A **22**, 3155 (2007).
[5] M. Ibe, W. Nakano, Y. Shoji, and K. Suzuki, J. High Energy Phys. 03 (2018) 194.
[6] E. Aprile *et al.* (XENON Collaboration), Phys. Rev. Lett. **123**, 241803 (2019).
[7] J. Tiffenberg, M. Sofo-Haro, A. Drlica-Wagner, R. Essig, Y. Guardincerri, S. Holland, T. Volansky, and T.-T. Yu

(SENSEI Collaboration), Phys. Rev. Lett. **119**, 131802 (2017).
[8] L. Barak, I. M. Bloch, M. Cababie, G. Cancelo, L. Chaplinsky *et al.* (SENSEI Collaboration), Phys. Rev. Lett. **125**, 171802 (2020).
[9] E. Aprile *et al.* (XENON Collaboration), Phys. Rev. Lett. **123**, 251801 (2019).
[10] Y. Hochberg, Y. F. Kahn, R. K. Leane, S. Rajendran, K. Van Tilburg, T.-T. Yu, and K. M. Zurek, Nat. Rev. Phys. **4**, 637 (2022).
[11] Y. Hochberg, Y. Zhao, and K. M. Zurek, Phys. Rev. Lett. **116**, 011301 (2016).
[12] Y. Hochberg, M. Pyle, Y. Zhao, and K. M. Zurek, J. High Energy Phys. 08 (2016) 057.
[13] Y. Hochberg, Y. Kahn, N. Kurinsky, B. V. Lehmann, T. C. Yu, and K. K. Berggren, Phys. Rev. Lett. **127**, 151802 (2021).
[14] Y. Hochberg, E. D. Kramer, N. Kurinsky, and B. V. Lehmann, Phys. Rev. D **107**, 076015 (2023).
[15] Y. Hochberg, I. Charaev, S.-W. Nam, V. Verma, M. Colangelo, and K. K. Berggren, Phys. Rev. Lett. **123**, 151802 (2019).
[16] J. Chiles *et al.*, Phys. Rev. Lett. **128**, 231802 (2022).
[17] K. Schutz and K. M. Zurek, Phys. Rev. Lett. **117**, 121302 (2016).
[18] S. Knapen, T. Lin, and K. M. Zurek, Phys. Rev. D **95**, 056019 (2017).
[19] A. Caputo, A. Esposito, and A. D. Polosa, Phys. Rev. D **100**, 116007 (2019).
[20] S. Griffin, S. Knapen, T. Lin, and K. M. Zurek, Phys. Rev. D **98**, 115034 (2018).
[21] S. Knapen, T. Lin, M. Pyle, and K. M. Zurek, Phys. Lett. B **785**, 386 (2018).
[22] P. Cox, T. Melia, and S. Rajendran, Phys. Rev. D **100**, 055011 (2019).
[23] M.-A. Sánchez-Martínez, I. n. Robredo, A. Bidauzarraga, A. Bergara, F. de Juan, A. G. Grushin, and M. G. Vergniory, Materials **3**, 014001 (2019).
[24] Y. Hochberg, Y. Kahn, M. Lisanti, K. M. Zurek, A. G. Grushin, R. Ilan, S. M. Griffin, Z.-F. Liu, S. F. Weber, and J. B. Neaton, Phys. Rev. D **97**, 015004 (2018).
[25] R. M. Geilhufe, B. Olsthoorn, A. Ferella, T. Koski, F. Kahlhoefer, J. Conrad, and A. V. Balatsky, Phys. Status Solidi RRL **12**, 1800293 (2018).
[26] R. M. Geilhufe, F. Kahlhoefer, and M. W. Winkler, Phys. Rev. D **101**, 055005 (2020).
[27] A. Coskuner, A. Mitridate, A. Olivares, and K. M. Zurek, Phys. Rev. D **103**, 016006 (2021).
[28] D. A. Neufeld, G. R. Farrar, and C. F. McKee, Astrophys. J. **866**, 111 (2018).
[29] M. Pospelov and H. Ramani, Phys. Rev. D **103**, 115031 (2021).
[30] M. Pospelov, S. Rajendran, and H. Ramani, Phys. Rev. D **101**, 055001 (2020).
[31] S. Rajendran and H. Ramani, Phys. Rev. D **103**, 035014 (2021).
[32] X. Xu and G. R. Farrar, arXiv:2112.00707.
[33] D. Budker, P. W. Graham, H. Ramani, F. Schmidt-Kaler, C. Smorra, and S. Ulmer, PRX Quantum **3**, 010330 (2022).
[34] D. McKeen, M. Moore, D. E. Morrissey, M. Pospelov, and H. Ramani, Phys. Rev. D **106**, 035011 (2022).
[35] J. Billard, M. Pyle, S. Rajendran, and H. Ramani, arXiv:2208.05485.
[36] R. K. Leane and J. Smirnov, J. Cosmol. Astropart. Phys. 10 (2023) 057.
[37] Y. Kahn and T. Lin, Rep. Prog. Phys. **85**, 066901 (2022).
[38] T. Trickle, Z. Zhang, K. M. Zurek, K. Inzani, and S. M. Griffin, J. High Energy Phys. 03 (2020) 036.
[39] S. Knapen, J. Kozaczuk, and T. Lin, Phys. Rev. D **105**, 015014 (2022).
[40] B. Campbell-Deem, S. Knapen, T. Lin, and E. Villarama, Phys. Rev. D **106**, 036019 (2022).
[41] D. Ristè, C. C. Bultink, M. J. Tiggelman, R. N. Schouten, K. W. Lehnert, and L. Dicarlo, Nat. Commun. **4**, 1913 (2013).
[42] P. M. Echternach, B. J. Pepper, T. Reck, and C. M. Bradford, Nat. Astron. **2**, 90 (2018).
[43] C. W. Fink, S. L. Watkins, T. Aramaki, P. L. Brink, J. Camilleri, X. Defay, S. Ganjam, Y. G. Kolomensky, R. Mahapatra, N. Mirabolfathi, W. A. Page, R. Partridge, M. Platt, M. Pyle, B. Sadoulet, B. Serfass, and S. Zuber, Appl. Phys. Lett. **118**, 022601 (2021).
[44] R. Ren *et al.*, Phys. Rev. D **104**, 032010 (2021).
[45] S. B. Kaplan, C. C. Chi, D. N. Langenberg, J. J. Chang, S. Jafarey, and D. J. Scalapino, Phys. Rev. B **14**, 4854 (1976).
[46] A. Bespalov, M. Houzet, J. S. Meyer, and Y. V. Nazarov, Phys. Rev. Lett. **117**, 117002 (2016).
[47] See Supplemental Material at http://link.aps.org/supplemental/10.1103/PhysRevLett.132.121801 for additional discussion of our inputs and results.
[48] J. F. Acevedo, R. K. Leane, and J. Smirnov, arXiv:2303.01516.
[49] E. O. Nadler *et al.* (DES Collaboration), Phys. Rev. Lett. **126**, 091101 (2021).
[50] K. K. Rogers, C. Dvorkin, and H. V. Peiris, Phys. Rev. Lett. **128**, 171301 (2022).
[51] W. L. Xu, C. Dvorkin, and A. Chael, Phys. Rev. D **97**, 103530 (2018).
[52] G. Angloher *et al.* (CRESST Collaboration), Eur. Phys. J. C **77**, 637 (2017).
[53] I. Alkhatib *et al.* (SuperCDMS Collaboration), Phys. Rev. Lett. **127**, 061801 (2021).
[54] E. Armengaud, C. Augier, A. Benoit, A. Benoit, L. Berge *et al.* (EDELWEISS Collaboration), Phys. Rev. D **99**, 082003 (2019).
[55] M. S. Mahdawi and G. R. Farrar, J. Cosmol. Astropart. Phys. 10 (2018) 007.
[56] F. Petricca *et al.* (CRESST Collaboration), J. Phys. Conf. Ser. **1342**, 012076 (2020).
[57] R. Agnese *et al.* (SuperCDMS Collaboration), Phys. Rev. D **97**, 022002 (2018).
[58] D. S. Akerib *et al.* (LUX Collaboration), Phys. Rev. Lett. **118**, 021303 (2017).
[59] E. Aprile *et al.* (XENON Collaboration), Phys. Rev. Lett. **119**, 181301 (2017).
[60] X. Cui *et al.* (PandaX-II Collaboration), Phys. Rev. Lett. **119**, 181302 (2017).
[61] D. Hooper and S. D. McDermott, Phys. Rev. D **97**, 115006 (2018).

[62] M. C. Digman, C. V. Cappiello, J. F. Beacom, C. M. Hirata, and A. H. G. Peter, Phys. Rev. D **100**, 063013 (2019).
[63] X. Xu and G. R. Farrar, Phys. Rev. D **107**, 095028 (2023).
[64] E. T. Mannila, P. Samuelsson, S. Simbierowicz, J. T. Peltonen, V. Vesterinen, L. Grönberg, J. Hassel, V. F. Maisi, and J. P. Pekola, Nat. Phys. **18**, 145 (2021).
[65] A. Vepsalainen *et al.*, Nature (London) **584**, 551 (2020).
[66] L. Cardani *et al.*, Nat. Commun. **12**, 2733 (2021).
[67] C. D. Wilen *et al.*, Nature (London) **594**, 369 (2021).
[68] J. M. Martinis, npj Quantum Inf. **7**, 90 (2021).